



Effects of MHD Maxwell Nanofluid Over a Stretching Sheet with Presence of Chemical Reaction and Heat Source/Sink.

N.Prabhudeva^{a*}

^aDepartment of Engineering Mathematics, Proudha Devaraya Institute of Technology, T.B. Dam, Hosapete, Karnataka, 583225, INDIA.

Abstract:

In this article, an attempt has been made to study the heat transfer characteristics of Maxwell-nanofluid flow over a stretching sheet with transverse magnetic field in the presence of chemical reaction. The nonlinear governing equations with suitable boundary conditions are initially cast into dimensionless form by similarity transformations and then the resulting highly nonlinear coupled partial differential equations are solved via (try use another word) the optimal homotopy analysis method. The impact of all sundry parameters like, Magnetic parameter, Deborah number, Prandtl number, Schmidt number, Rotation parameter, Velocity slip parameter, Chemical reaction parameter, Thermophoresis parameter, Brownian motion parameter, Heat sources per sink parameter, Biot number, Eckert number on the velocity, temperature and concentration field are analyzed through graphs and tables.

Keywords: Nanofluid; Heat source/sink; Velocity slip; Chemical Reaction.

Introduction

Over the decades, the study of boundary layer flow and heat transfer over a stretching sheet has (drawn) attracted the attention of several researchers due to its various industrial and engineering applications such as, annealing and tinning of copper wires, manufacturing of plastic and rubber sheets, crystal growing, continuous cooling, extrusion of polymer, wire drawing, in textiles and glass fiber production, paper production etc. In view of these applications, beginning with the pioneering work by (These lines are not necessary or sentence not in proper order) Sakiadis [1] initiated the study of boundary layer flow past a stretching surface. Crane [2] examined the flow and heat transfer characteristics of Sakiadis' flow. The significance of heat transfer over a continuous stretching surface with variable temperature is mentioned in ref [3-4].

Many researchers at present are engaged in exploring the flows of non-Newtonian fluids at various aspects. Non-Newtonian fluids are very popular due to their importance (please rewrite this sentence) in our daily life. Examples of such fluids include, sugar solutions, tomato ketchup, lubricants, apple sauce, shampoos, cosmetic products, and many others. The non-Newtonian fluids frequently appear in industry and in

engineering (Try to add few more areas here). Due to the distinct physical structures of fluids, that can describe all the rheological properties of such fluids. In spite of this, the non-Newtonian fluids have been classified into three types: (i) the differential type, (ii) the rate type and (iii) the integral type. There is a simplest subclass of rate type fluids known as (once you verify this line) upper-convected Maxwell (UCM) fluid. This model can easily predict the relaxation time phenomena. Recent contribution on the flow analysis of UCM fluid include those of Abbas et al. [5], Hayat et al. [6], Abel et al. [7], Nadeem et al. [8], Awasi et al. [9], Shafique et al. [10]. In recent years, some interest has been given to analyze the convective transport of nanofluids. Its main advantage is thermal conductivity of the fluids plays an important role on the heat transfer coefficient between the heat transfer medium and heat transfer surface. Nano-scale particles added fluids are called nanofluid, which is firstly coined by Choi [11]. Choi was the finally revealed to the society about the enhancement of thermal conductivity of fluids with nanoparticle. Many researchers investigated an excellent work on nanofluid over a stretching sheet with distinct physical aspects such as presence of magnetic field, slip effect condition, convective heat transfer and viscous dissipation. (Rearrange properly this sentence) Examined the boundary layer flow of a nanofluid past a stretching sheet with a convective boundary condition Ref. [12-13]. Study of convective heat transfer in the flow of viscous Ag-water and Cu-water nanofluid over a stretching surface excellent work done by Vajravelu et al. [14].

The study of heat generation and absorption on heat transfer is very important because its effects are crucial in controlling the heat transfer. Bataller [15] explained the heat transfer of a viscoelastic fluid over a stretching sheet in the presence of heat source/sink. Ramesh and Gireesha [16] explore the importance of heat source/sink on a Maxwell fluid over a stretching sheet with convective boundary condition in the presence of nanoparticles. Several researchers investigated the effect of viscous dissipation and heat generation and absorption over a stretching sheet and shrinking sheet Ref. [17-19]. (Try to change starting words of this sentence) In above cited papers they are shown that for effective cooling of stretching, heat source/sink should used. Andersson [20] examined the slip flow past a stretching sheet. Ibrahim and Shankar [21] studied the MHD boundary layer flow and heat transfer of a nanofluid past a permeable stretching sheet with velocity slip. Sui et al. [22] investigated the effect of heat and mass transfer with cattaneo-christov double-diffusion in UCM nanofluid past a stretching sheet with slip velocity. Rout et al. [23] reported the heat and mass transfer of chemical reaction fluid flow over a moving vertical plate in presence of magnetic field with heat source and convective surface boundary condition. Anjanna Matta and Nagaraju Gajjela [24] numerically studied the order of chemical reaction and convective boundary condition effects on micropolar fluid flow over a stretching sheet.

In this article, to explore the influences of magnetic field and heat source/sink on rotating flow of non-Newtonian Maxwell nanofluid over an stretching surface with chemical reaction and velocity slip. The governing nonlinear coupled (partial differential) system of equations for flow and heat transfer have been lessened to nonlinear coupled differential equations are solved by Optimal Homotopy Analysis Method (OHAM) [25-26]. Solutions for Horizontal velocity, transverse velocity, temperature distribution and concentration distribution are developed. Pictorial illustrations for Horizontal velocity, transverse velocity, temperature and concentration are presented to emphasize the physical effects of sundry parameters on the solutions. Numerical values of Horizontal skin friction, transverse skin friction, local Nusselt number and local Sherwood number for a range of parameters are tabulated.

1. Mathematical Modeling of the Problem

Consider a three-dimensional, steady boundary layer flow of a viscous incompressible non-Newtonian Maxwell-nanofluid by an elastic surface subjected to the convective boundary condition and zero mass flux nanoparticle concentration. A Cartesian coordinate system is chosen such that the surface is stretched in the x -direction with linearly varying velocity of the form $u_w(x) = ax + \lambda \frac{\partial u}{\partial z}$ which induces flow in the neighboring layers of the fluid. The uniform magnetic flux B_0 is acting along y -axis. Let Ω be the constant angular velocity of the rotating fluid. Geometry of the problem is shown in below Fig.1.

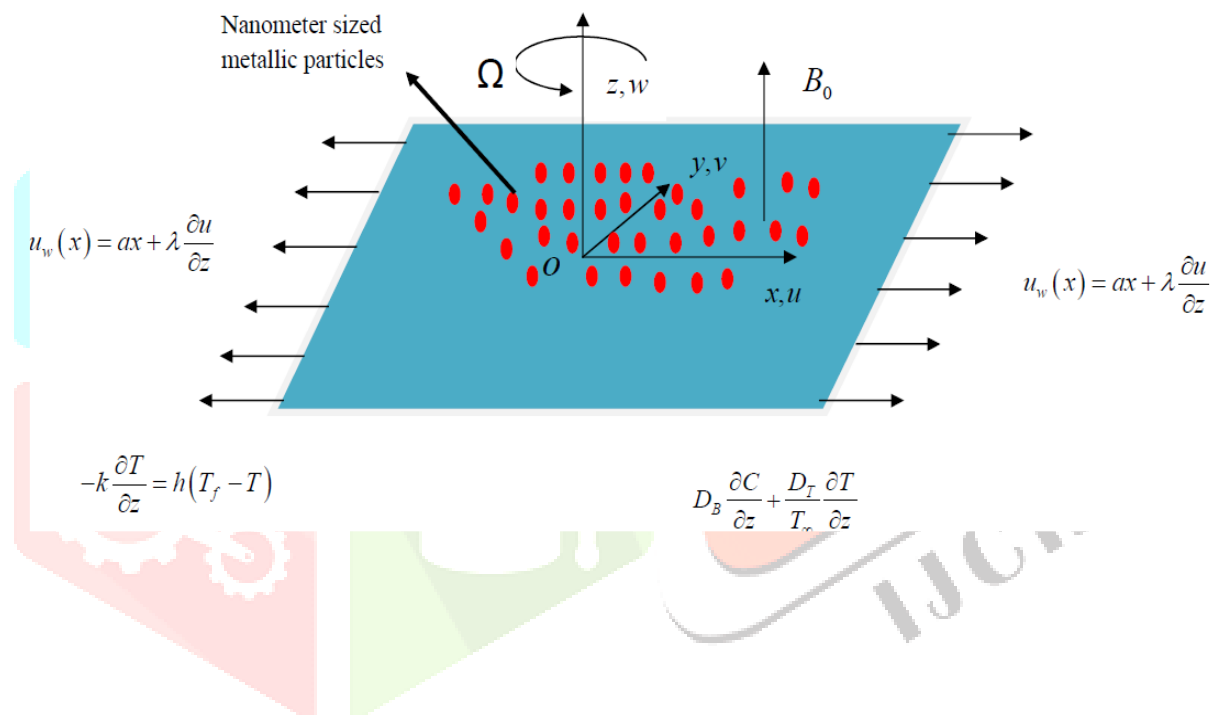


Fig.1: Schematic diagram and coordinate system

The problem under consideration is governed by the following boundary layer equations of Maxwell fluid along nano-particles in the presence of heat source per sink and chemical reaction which are given by

$$\frac{\partial u}{\partial x} + \frac{\partial v}{\partial y} + \frac{\partial w}{\partial z} = 0 \quad (1)$$

$$u \frac{\partial u}{\partial x} + v \frac{\partial u}{\partial y} + w \frac{\partial u}{\partial z} - 2\Omega v = \nu \left(\frac{\partial^2 u}{\partial z^2} \right) - \lambda_1 \left[u^2 \frac{\partial^2 u}{\partial x^2} + v^2 \frac{\partial^2 u}{\partial y^2} + w^2 \frac{\partial^2 u}{\partial z^2} + 2uv \frac{\partial^2 u}{\partial x \partial y} + 2vw \frac{\partial^2 u}{\partial y \partial z} + 2uw \frac{\partial^2 u}{\partial x \partial z} - 2\Omega \left(u \frac{\partial v}{\partial x} + v \frac{\partial v}{\partial y} + w \frac{\partial v}{\partial z} \right) + 2\Omega \left(v \frac{\partial u}{\partial x} - u \frac{\partial u}{\partial y} \right) \right] - \frac{\sigma B_0^2}{\rho} \left[u + \lambda_1 w \frac{\partial u}{\partial z} \right] \quad (2)$$

$$u \frac{\partial v}{\partial x} + v \frac{\partial v}{\partial y} + w \frac{\partial v}{\partial z} - 2\Omega u = \nu \left(\frac{\partial^2 v}{\partial z^2} \right) - \lambda_1 \left[u^2 \frac{\partial^2 v}{\partial x^2} + v^2 \frac{\partial^2 v}{\partial y^2} + w^2 \frac{\partial^2 v}{\partial z^2} + 2uv \frac{\partial^2 v}{\partial x \partial y} + 2vw \frac{\partial^2 v}{\partial y \partial z} + 2uw \frac{\partial^2 v}{\partial x \partial z} + 2\Omega \left(u \frac{\partial u}{\partial x} + v \frac{\partial u}{\partial y} + w \frac{\partial u}{\partial z} \right) + 2\Omega \left(v \frac{\partial v}{\partial x} - u \frac{\partial v}{\partial y} \right) \right] - \frac{\sigma B_0^2}{\rho} \left[v + \lambda_1 w \frac{\partial v}{\partial z} \right] \quad (3)$$

$$u \frac{\partial T}{\partial x} + v \frac{\partial T}{\partial y} + w \frac{\partial T}{\partial z} = \alpha \frac{\partial^2 T}{\partial z^2} + \frac{Q}{\rho C_p} (T - T_\infty) + \frac{\mu}{\rho C_p} \left[\left(\frac{\partial u}{\partial z} \right)^2 + \left(\frac{\partial v}{\partial z} \right)^2 \right] + \left\{ \tau \left[D_B \left(\frac{\partial T}{\partial z} \cdot \frac{\partial C}{\partial z} \right) + \frac{DT}{T_\infty} \left(\frac{\partial T}{\partial z} \right)^2 \right] \right\} \quad (4)$$

$$u \frac{\partial C}{\partial x} + v \frac{\partial C}{\partial y} + w \frac{\partial C}{\partial z} = D_B \left[\frac{\partial^2 C}{\partial z^2} \right] + \frac{D_T}{T_\infty} \left[\frac{\partial^2 T}{\partial z^2} \right] - k_1 [C - C_\infty] \quad (5)$$

where u , v and w are the fluid velocity components in the x , y and z directions respectively.

The appropriate boundary conditions are given as:

$$u = u_w(x) = ax + k_1 \frac{\partial u}{\partial z}, \quad v = 0, \quad w = 0, \\ -k \frac{\partial T}{\partial z} = h_f (T_f - T), \quad D_B \frac{\partial C}{\partial z} + \frac{D_T}{T_\infty} \frac{\partial T}{\partial z} = 0 \quad \text{at } z = 0, \quad (6) \\ u \rightarrow 0, \quad v \rightarrow 0, \quad T \rightarrow T_\infty, \quad C \rightarrow C_\infty \quad \text{as } z \rightarrow \infty.$$

Introducing the following

set of dimensionless similarity transformations

$$\eta = \sqrt{\frac{a}{\nu}} z, \quad u = axf'(\eta), \quad v = axg(\eta), \quad w = -\sqrt{av}f(\eta), \\ \theta = \frac{T - T_\infty}{T_w - T_\infty}, \quad \phi = \frac{C - C_\infty}{C_w - C_\infty}, \quad (7) \text{ Using the Eq. (7),}$$

we observe that Eq. (1) is satisfied. Substituting these transformations into (2) to (5) by simplification can be presented as

$$f''' + ff'' - f'^2 + 2\lambda[g - \beta fg'] + \beta[2f''f' - f^2 f'''] - Mn[f' - \beta ff''] = 0 \quad (8)$$

$$g'' + fg' - f'g - 2\lambda[f' + \beta(f'^2 - ff'' + g^2)] + \beta[2ff'g' - f^2 g''] - Mn[g - \beta fg'] = 0 \quad (9)$$

$$\frac{1}{Pr}\theta'' + f\theta' + \alpha\theta + Ec[f'^2 + g'^2] + Nb\theta'\phi' + Nt\theta'^2 = 0 \quad (10)$$

$$\phi'' + Scf\phi' + \left(\frac{Nt}{Nb}\right)\theta'' - Sc\delta\phi = 0 \quad (11)$$

Subjected to the transformed conditions

$$\begin{aligned} \text{at } \eta \rightarrow 0: \quad f(0) = g(0) = 0, \quad f'(0) = 1 + Kf''(0), \\ \theta'(0) = -\gamma[1 - \theta(0)], \quad Nb\phi'(0) + Nt\theta'(0) = 0. \\ \text{as } \eta \rightarrow \infty: \quad f'(\infty) = g(\infty) = \theta(\infty) = \phi(\infty) = 0. \end{aligned} \quad (12) \quad \text{Where the non-}$$

dimensional quantities like $Mn, \beta, \lambda, Pr, \alpha, Ec, Sc, \delta, Nt, Nb, K$ and γ are respectively the Magnetic number, Deborah number, Rotation parameter, Prandtl number, Heat source sink parameter, Eckert number, Schmidt number, Chemical reaction, Thermophoresis parameter, Brownian motion parameter, Velocity slip parameter and Biot number are defined as follows:

$$\begin{aligned} Mn = \frac{\sigma B_0^2}{\rho a}, \quad \beta = \lambda_1 a, \quad \lambda = \frac{\Omega}{a}, \quad Pr = \frac{\alpha}{\nu}, \quad K = k_1 \sqrt{\frac{a}{\nu}}, \\ \alpha = \frac{Q}{\rho c_p a}, \quad Ec = \frac{a^2 x^2}{c_p (T_w - T_\infty)}, \quad Sc = \frac{\nu}{D_B}, \quad \gamma = \frac{h}{k} \sqrt{\frac{\nu}{a}}, \\ \delta = \frac{k_c}{a}, \quad Nb = \frac{\tau D_B}{\nu} (c_w - c_\infty), \quad Nt = \frac{\tau D_T}{T_\infty \nu} (T_w - T_\infty). \end{aligned} \quad (13) \quad \text{The quantities}$$

with core physical interest are by using Fourier law can be to define local Nusselt number Nu_x and Fick's law can be used to define local Sherwood number Sh_x . These are as follows:

$$Nu_x = \frac{xq_w}{k(T_w - T_\infty)}, \quad Sh_x = \frac{xj_w}{D(C_w - C_\infty)} \quad (14) \quad \text{where } q_w \text{ is the}$$

wall heat flux and j_w is the wall mass flux given by

$$q_w = -k \left. \frac{\partial T}{\partial z} \right|_{z=0}, \quad j_w = -D \left. \frac{\partial C}{\partial z} \right|_{z=0} \quad (15) \quad \text{Now using Eq.}$$

(7) and Eq. (14), Eq. (15) becomes

$$\frac{Nu_x}{\sqrt{Re_x}} = -\theta'(0), \quad \frac{Sh_x}{\sqrt{Re_x}} = -\phi'(0), \quad (16) \quad \text{where}$$

$Re_x = ax^2/\nu$ is the local Reynolds number.

2. Method of solution

OHAM is semi-analytical method, which is totally based on the concept of homotopy, it's derived from topology. OHAM plays an important tool where a non-linear problem is transformed into an infinite number of linear sub-problems. Which is much easier to solve than the non-linear ones in this view we have following steps as follows:

We choose the auxiliary linear operators as

$$L_f = \frac{d^3}{d\eta^3} - \frac{d}{d\eta}, \quad L_g = \frac{d^2}{d\eta^2} - f, \quad L_\theta = \frac{d^2}{d\eta^2} - f, \quad L_\phi = \frac{d^2}{d\eta^2} - f, \quad (17)$$

Initial approximations satisfying the boundary conditions (6) are found to be

$$f_0(\eta) = \left(\frac{1}{1+K} \right) (1 - e^{-\eta}), \quad g_0(\eta) = 0,$$

$$\theta_0(\eta) = \left(\frac{\gamma}{1+\gamma} \right) e^{-\eta}, \quad \phi_0(\eta) = \left(\frac{-\gamma}{1+\gamma} \right) \left(\frac{Nt}{Nb} \right) e^{-\eta},$$

Let us consider the so-called zeroth order deformation equations.

$$(1-q)L_f [\hat{f}(\eta;q) - f_0(\eta)] = qH_f(\eta)h_f N_f [\hat{f}(\eta;q), \hat{g}(\eta;q)] \quad (18)$$

$$(1-q)L_g [\hat{g}(\eta;q) - g_0(\eta)] = qH_g(\eta)h_g N_g [\hat{g}(\eta;q), \hat{f}(\eta;q)] \quad (19)$$

$$(1-q)L_\theta [\hat{\theta}(\eta;q) - \theta_0(\eta)] = qH_\theta(\eta)h_\theta N_\theta [\hat{\theta}(\eta;q), \hat{f}(\eta;q), \hat{g}(\eta;q), \hat{\phi}(\eta;q)] \quad (20)$$

$$(1-q)L_\phi [\hat{\phi}(\eta;q) - \phi_0(\eta)] = qH_\phi(\eta)h_\phi N_\phi [\hat{\phi}(\eta;q), \hat{f}(\eta;q), \hat{\theta}(\eta;q)] \quad (21)$$

Here $q \in [0,1]$ is an embedding parameter, while $h_f \neq 0, h_g \neq 0, h_\theta \neq 0$, and $h_\phi \neq 0$ are the convergence control parameters, and the nonlinear differential operators.

$$N_f [\hat{f}, \hat{g}] = \frac{\partial^3 \hat{f}}{\partial \eta^3} + \hat{f} \frac{\partial^2 \hat{f}}{\partial \eta^2} - \left(\frac{\partial \hat{f}}{\partial \eta} \right) + 2\lambda \left[\hat{g} - \beta \hat{f} \frac{\partial \hat{g}}{\partial \eta} \right]$$

$$+ \beta \left[2 \frac{\partial^2 \hat{f}}{\partial \eta^2} \frac{\partial \hat{f}}{\partial \eta} \hat{f} - \hat{f}^2 \frac{\partial^3 \hat{f}}{\partial \eta^3} \right] - Mn \left[\frac{\partial \hat{f}}{\partial \eta} - \beta \hat{f} \frac{\partial^2 \hat{f}}{\partial \eta^2} \right] \quad (22)$$

$$N_g [\hat{f}, \hat{g}] = \frac{\partial^2 \hat{g}}{\partial \eta^2} + \hat{f} \frac{\partial \hat{g}}{\partial \eta} - \frac{\partial \hat{f}}{\partial \eta} \hat{g} - 2\lambda \left[\frac{\partial \hat{f}}{\partial \eta} + \beta \left(\left(\frac{\partial \hat{f}}{\partial \eta} \right)^2 - \hat{f} \frac{\partial^2 \hat{f}}{\partial \eta^2} + \hat{g}^2 \right) \right]$$

$$+ \beta \left[2 \hat{f} \frac{\partial \hat{f}}{\partial \eta} \frac{\partial \hat{g}}{\partial \eta} - \hat{f}^2 \frac{\partial^2 \hat{g}}{\partial \eta^2} \right] - Mn \left[\hat{g} - \beta \hat{f} \frac{\partial \hat{g}}{\partial \eta} \right] \quad (23)$$

$$N_\theta \left[\hat{f}, \hat{g}, \hat{\theta}, \hat{\phi} \right] = \frac{\partial^2 \hat{\theta}}{\partial \eta^2} + \text{Pr} \hat{f} \frac{\partial \hat{\theta}}{\partial \eta} + \text{Pr} \alpha_1 \hat{\theta} + \text{Pr} Ec \left[\left(\frac{\partial^2 \hat{f}}{\partial \eta^2} \right)^2 + \left(\frac{\partial \hat{g}}{\partial \eta} \right)^2 \right] \quad (24)$$

$$+ Nb \text{Pr} \frac{\partial \hat{\theta}}{\partial \eta} \frac{\partial \hat{\phi}}{\partial \eta} + \text{Pr} Nt \left(\frac{\partial \hat{\theta}}{\partial \eta} \right)^2$$

$$N_\phi \left[\hat{f}, \hat{\theta}, \hat{\phi} \right] = \frac{\partial^2 \hat{\phi}}{\partial \eta^2} + Sc \hat{f} \frac{\partial \hat{\phi}}{\partial \eta} + \left(\frac{Nt}{Nb} \right) \frac{\partial^2 \theta}{\partial \eta} - Sc \delta \hat{\phi} \quad (25)$$

3. Results and discussion

In this article, the system of Eq. (8) to Eq. (11) are highly non-linear and coupled ordinary differential equations. Exact analytical solutions for the complete set of equations subject to the boundary conditions (12) are solved analytically via efficient OHAM. The results are demonstrated through pictorially and tabular form. Figures are drawn for Horizontal velocity $f'(\eta)$, Transverse velocity $g(\eta)$, temperature field $\theta(\eta)$ and concentration field $\phi(\eta)$. The impact of the physical sundry parameters such as the magnetic parameter Mn , the Deborah number β , the rotation parameter λ , the Prandtl number Pr , the heat sources sink parameter α , the Biot number γ , the Eckert number Ec , the Schmidt number Sc , the chemical reaction δ , the velocity slip parameter K , the thermophoresis parameter Nt and Brownian motion parameter Nb on the $f'(\eta)$, $g(\eta)$, $\theta(\eta)$ and $\phi(\eta)$ are analyzed graphically in Figures 2(a)-6(d). In Fig. 2(a-d) demonstrate the effect of increasing values of β and Mn on $f'(\eta)$, $g(\eta)$, $\theta(\eta)$ and $\phi(\eta)$ respectively. In Fig. 2(a) increasing β and Mn corresponds to decreases in the case of Horizontal velocity this is due to the fact that retarding force called the Lorentz force. But in the opposite trend is observed in the case of transverse velocity $g(\eta)$, temperature field $\theta(\eta)$ and concentration field $\phi(\eta)$ (see fig 2(b),2(c),2(d)). Reveals the effect of the rotation parameter λ and slip velocity parameter K with magnetic parameter Mn on Horizontal velocity profile respectively. The rotation effect seen in Fig.3(a) when the values of Mn and λ increasing it shows the velocity profile $f'(\eta)$ gradually decreasing in nature due to fact that by coriolis force. In Fig. 3(b) its shows that with the increasing values of Mn and K the fluid velocity decreases. i.e., a slip velocity occurs it is readily seen that K has a substantial effect on the Horizontal velocity profile. The effect of Pr and γ on temperature field is show in Fig.3(c). Here we noted that temperature field $\theta(\eta)$ increases rapidly near the boundary by increasing Biot number. Due to the fact that γ is directly proportional to the heat transfer coefficient h_f , since this substantial γ cause's stronger convection which leads increment in the temperature distribution. It also depicts that the temperature decreases when the values of Pr increases. The Prandtl number signifies the ratio of momentum diffusivity. This is since a higher Pr fluid has relatively low thermal conductivity, which reduces conduction and thereby the thermal boundary layer thickness, and as a result, thermal boundary layer thickness declined.

Here interested note that in heat transfer problems, the role of Prandtl number and heat sources/sink parameter controls the relative thickening of the momentum and the thermal boundary layers. Reveals the impact of different values of Ec and α on $\theta(\eta)$ can be found from Fig. 3(d). For increasing values of Ec and α increasing the thermal field. It is discussing in different cases for $\alpha > 0$ (heat generation), it can be observed that the thermal boundary layer generates the energy, and this causes the temperature in the thermal boundary layer increases with increases in α . Whereas $\alpha < 0$ (heat absorption) leads to decrease in the thermal boundary layer. When $\alpha = 0$ indicates the absence of heat sources/sink. Reveals the effect of Brownian motion parameter Nb and thermophoresis parameter Nt on $\theta(\eta)$ and $\phi(\eta)$ profiles as shown in the Fig.4(a-b) for increasing value of Nt , thickness of thermal boundary layer is increases whereas similar trend is recorded in the case of Nb (see Fig.4(a)). Fig.4(b) elucidates the effect of thermophoresis parameter decrease the concentration distribution whereas it is strengthened in the case of Brownian motion parameter.

Conclusion:

The following are the some of the important findings:

- ❖ For higher values of magnetic parameter and Deborah number, horizontal velocity field is declined.
- ❖ The effect of Thermophoresis and Brownian motion parameter enhances the thermal conductivity.
- ❖ Rotation parameter and velocity slip parameter opposes the fluid flow whereas decreasing pattern observed in the case of Horizontal velocity.
- ❖ For increasing values of Biot number and Heat source/sink parameter enhances the thermal boundary layer thickness.
- ❖ Concentration distribution is gradually enhancing for increasing values of Schmidt number and Chemical reaction.
- ❖ The effect of Eckert number enhances the thermal boundary layer thickness.

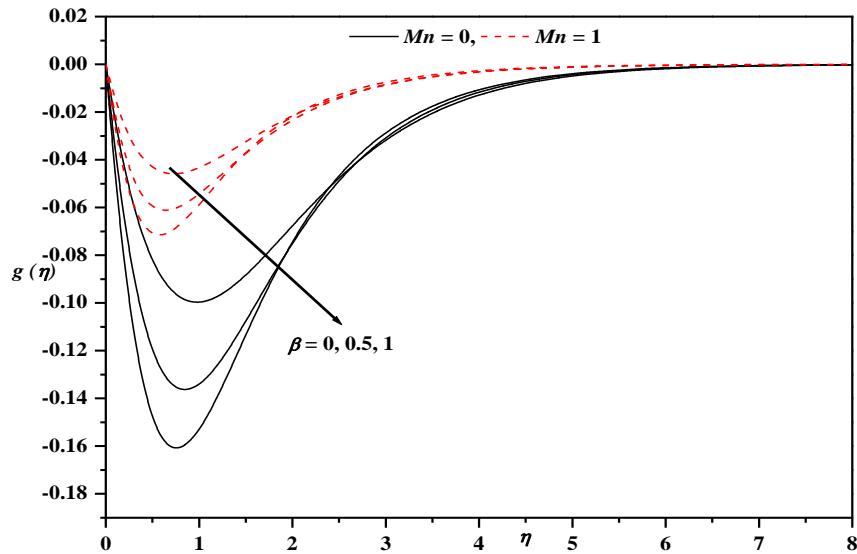


Fig.2(b): Transverse velocity profile for different values of Mn and β with $Pr = 1.09$
 $\gamma = 0.5, \lambda = 0.2, Nt = 0.3, Nb = 0.5, Ec = 0.02, \alpha = 0.1, Sc = 0.22, \delta = 0.5, K = 0.2$.

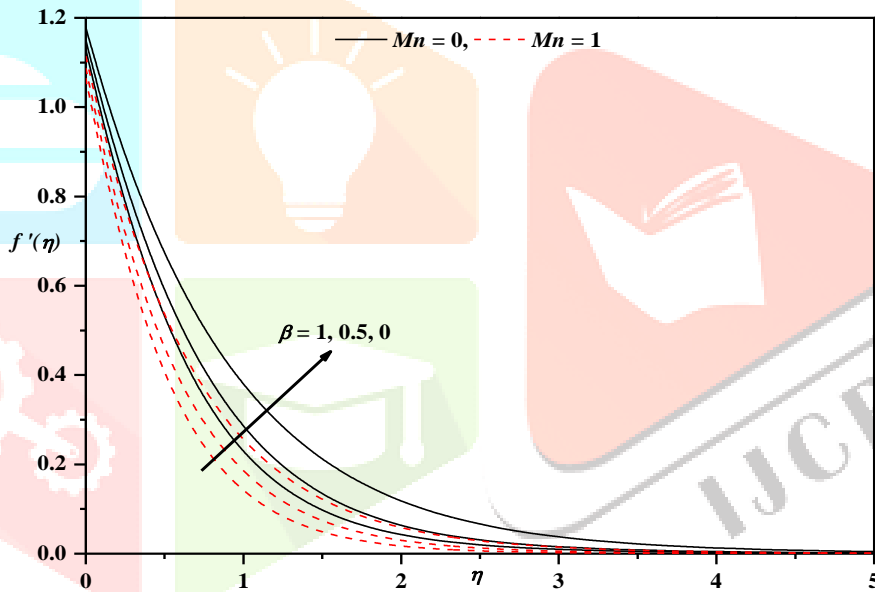


Fig.2(a): Horizontal velocity profile for different values of Mn and β with $Pr = 1.09$
 $\gamma = 0.5, \lambda = 0.2, Nt = 0.3, Nb = 0.5, Ec = 0.02, \alpha = 0.1, Sc = 0.22, \delta = 0.5, K = 0.2$.

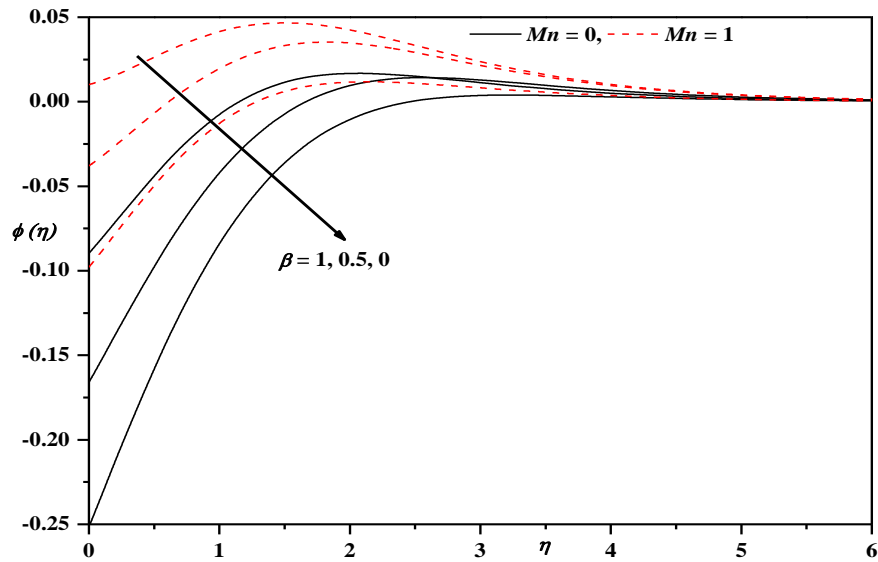


Fig.2(d): Concentration profile for different values of Mn and β with $Pr = 1.09$, $\gamma = 0.5$, $\lambda = 0.2$, $Nt = 0.3$, $Nb = 0.5$, $Ec = 0.02$, $\alpha = 0.1$, $Sc = 0.22$, $\delta = 0.5$, $K = 0.2$.

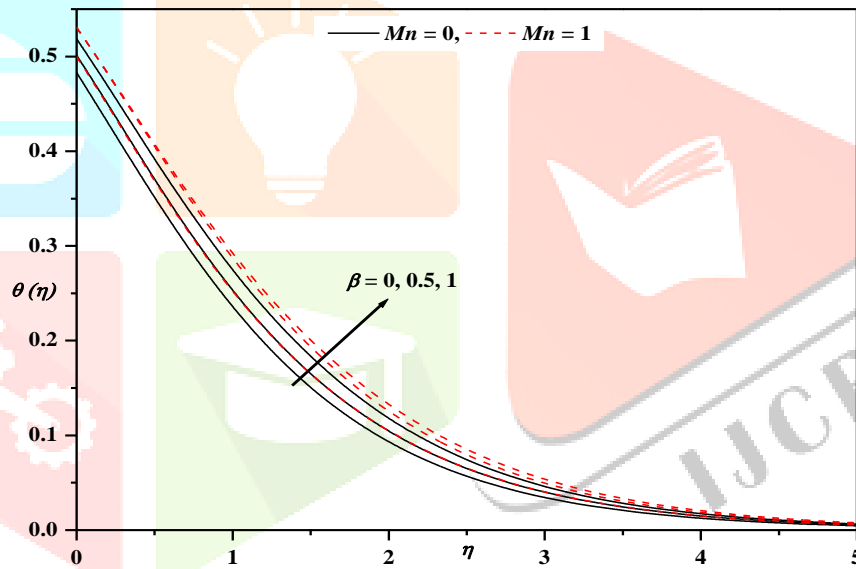


Fig.2(c): Temperature profile for different values of Mn and β with $Pr = 1.09$, $Ec = 0.02$, $\gamma = 0.5$, $\lambda = 0.2$, $Nt = 0.3$, $Nb = 0.5$, $\alpha = 0.1$, $Sc = 0.22$, $\delta = 0.5$, $K = 0.2$.

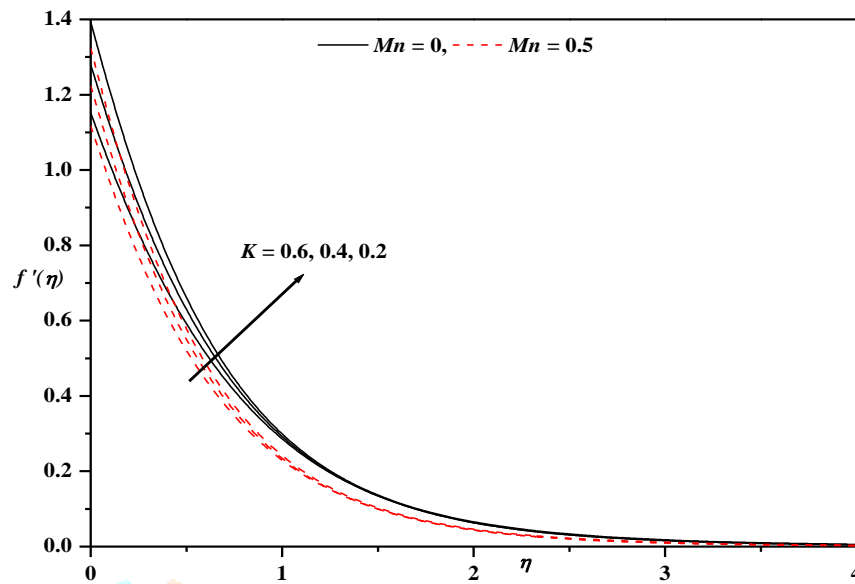


Fig.3(b):Horizontal velocity profile for different values of Mn and K with $Pr = 1.09$, $\gamma = 0.5$, $\lambda = 0.2$, $Nt = 0.3$, $Nb = 0.5$, $Ec = 0.02$, $\alpha = 0.1$, $Sc = 0.22$, $\delta = 0.5$, $\beta = 0.5$.

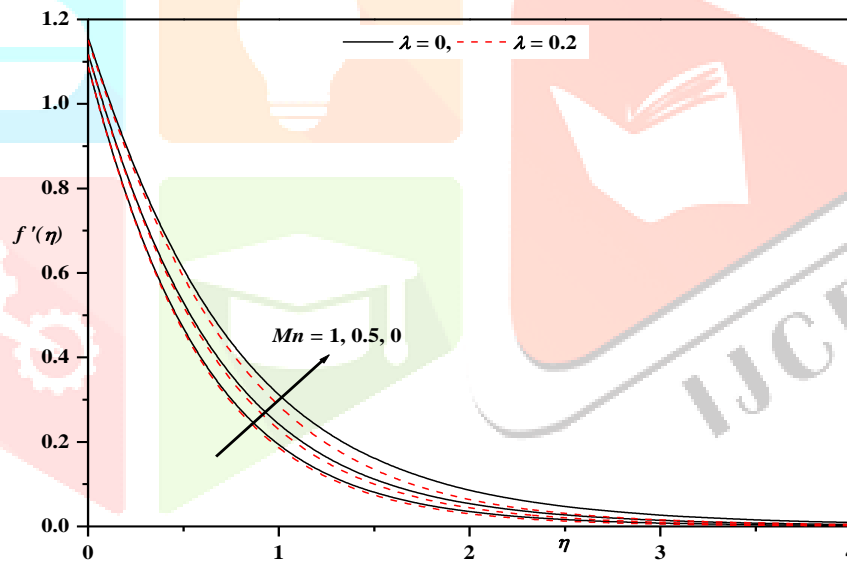


Fig.3(a):Horizontal velocity profile for different values of Mn and λ with $Pr = 1.09$, $\gamma = 0.5$, $\beta = 0.5$, $Nt = 0.3$, $Ec = 0.02$, $Nb = 0.5$, $\alpha = 0.1$, $Sc = 0.22$, $\delta = 0.5$, $K = 0.2$.

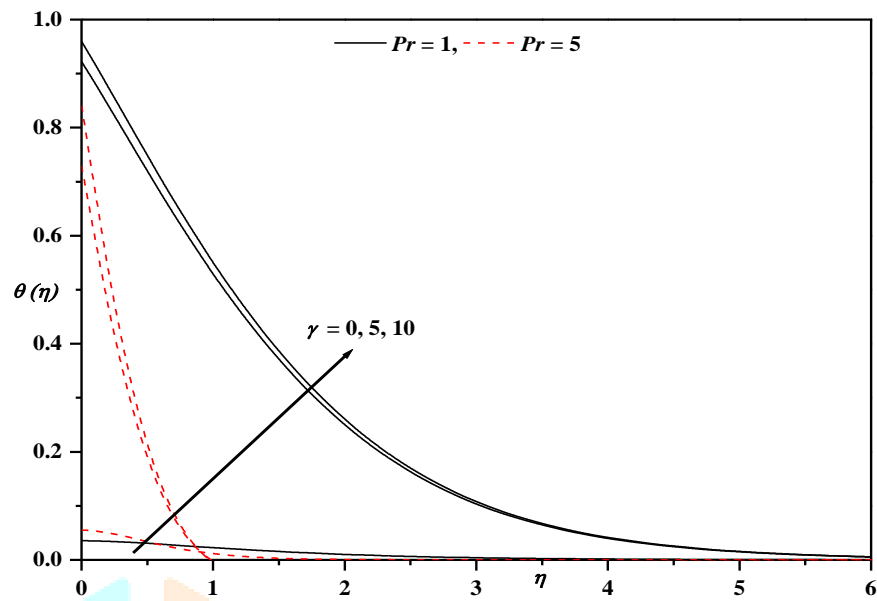


Fig.3(c): Temperature profile for different values of Pr and γ with $Mn = 0.5$, $\beta = 0.5$, $\lambda = 0.2$, $Nt = 0.3$, $Ec = 0.02$, $Nb = 0.5$, $\alpha = 0.1$, $Sc = 0.22$, $\delta = 0.5$, $K = 0.2$.

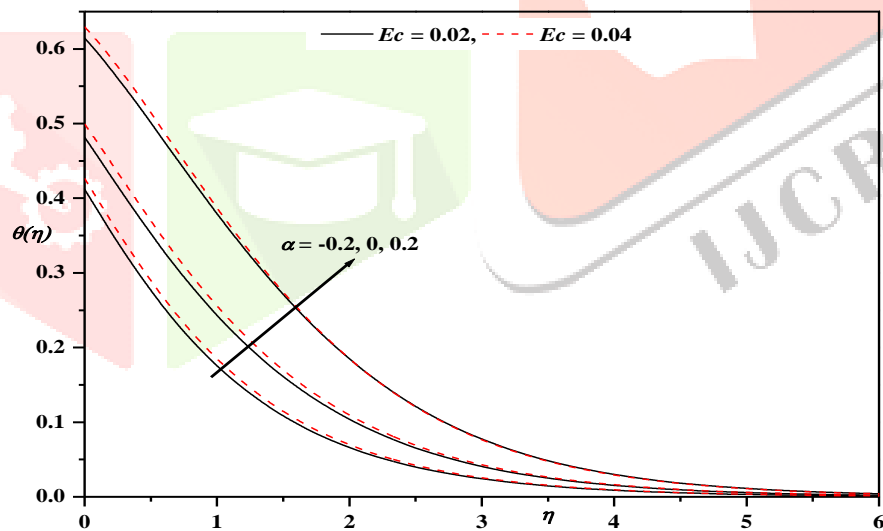


Fig.3(d): Temperature profile for different values of Ec and α with $Mn = 0.5$, $\beta = 0.5$, $\lambda = 0.2$, $Nt = 0.3$, $Pr = 1.09$, $Nb = 0.5$, $\gamma = 0.5$, $Sc = 0.22$, $\delta = 0.5$, $K = 0.2$.

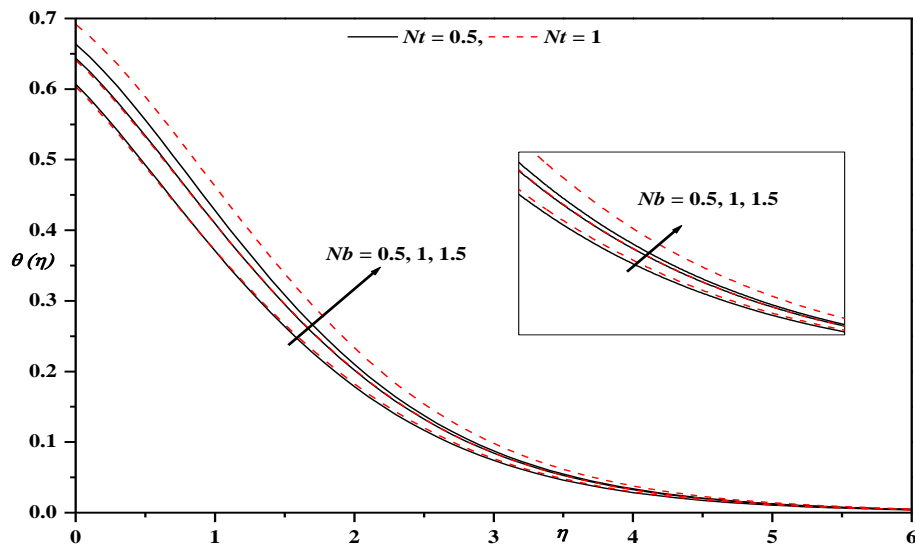


Fig.4(a): Temperature profile for different values of Nt and Nb with $Mn = 0.5$, $\beta = 0.5$, $\lambda = 0.2$, $\alpha = 0.2$, $Ec = 0.02$, $Pr = 1.09$, $\gamma = 0.5$, $Sc = 0.22$, $\delta = 0.5$, $K = 0.2$.

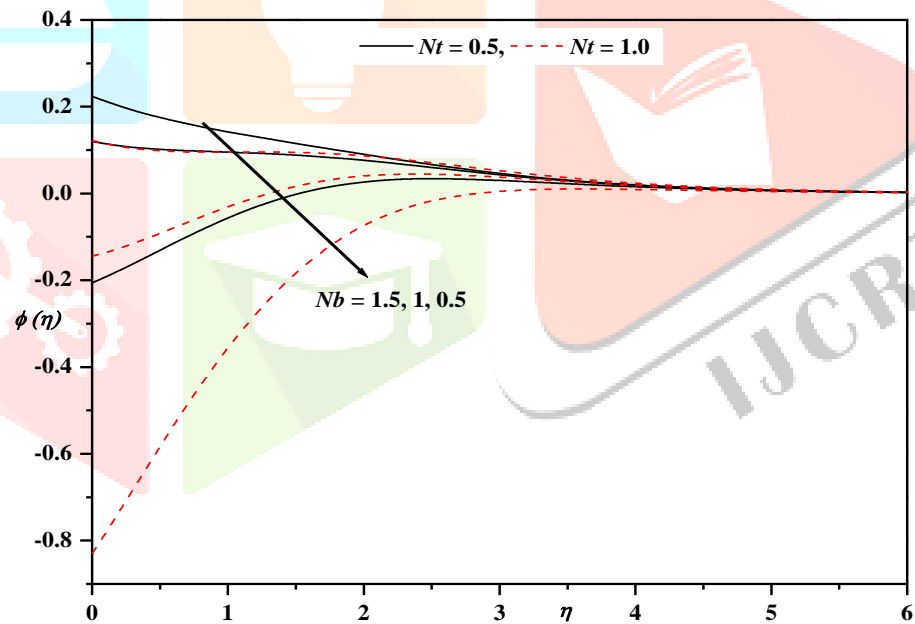


Fig.4(b): Concentration profile for different values of Nt and Nb with $Ec = 0.02$, $\beta = 0.5$, $\lambda = 0.2$, $\alpha = 0.2$, $Pr = 1.09$, $Mn = 0.5$, $\gamma = 0.5$, $Sc = 0.22$, $\delta = 0.5$, $K = 0.2$.

References

- [1]. B.C.Sakiadis, Boundary layer behavior on a continuous solid surface: I. Boundary layer equations for two dimensional and axisymmetric flow. *J. AIChE*. 7,26-28(1961).
- [2]. L.J.Crane, Flow past a stretching plate. *Z Angew Math Phys (ZAMP)*. 21(4),645-7(1970).
- [3]. Grubka LJ, bobba KM. Heat transfer characteristics of a continuous stretching surface with variable temperature. *J. Heat Transfer* 107,248-50(1985).
- [4]. C.K. Chen, M.I. Char, Heat transfer of a continuous stretching surface with suction or blowing. *J. Math. Anal. Appl.* vol. 135,568-580(1988).
- [5]. F.M. Abbasi, M. Mustafa, S.A. Shehzad, M.S. Alhuthali and T. Hayat, Analytical study of Cattaneo-Christov heat flux model for a boundary layer flow of oldroyd-B fluid. *Chin. Phys*,25(1),014701(2016).
- [6]. T. Hayat, M. Mustafa, S.A. Shehzad and S. Obaidat. Melting heat transfer in the stagnation point flow of an upper-convected Maxwell (UCM) fluid past a stretching sheet. *Int. j. Numer. Meth. Fluids* 68,233-243(2012).
- [7]. M. Subhas Abel, Jagadish V. Tawade and Mahantesh M. Nandeppanavar, MHD flow and heat transfer for the upper-convected Maxwell fluid over a stretching sheet. 47,385-393(2012).
- [8]. S. Nadeem, Rizwan UI Haq and Z.H. Khan, Numerical study of MHD boundary layer flow of a Maxwell fluid past a stretching sheet in the presence of nanoparticles. 45,121-126(2016).
- [9]. Muhammad Awais, Tasawar Hayat, Sania Irum and Ahmed Alsaedi, Heat generation/absorption effects in a boundary layer stretched flow of Maxwell Nanofluid: Analytic and Numeric Solutions. DOI:10.1371/journal.pone.0129814 june 26,(2015).
- [10]. Z.Shafique, M.Mustafa, A.Mushtaq. Boundary layer flow of Maxwell fluid in rotating frame with binary chemical reaction and activation energy. *Results in Physics* 6,627-633(2016).
- [11]. Choi S. Enhancing thermal conductivity of fluids with nanoparticle, In D.A.Siginer, H.P.Wang (Eds), *Developments and Applications of Non-Newtonian Flows*. ASME, MD 231 and FED,66,99-105(1995).
- [12]. W.A. Khan and I. Pop. Boundary-layer flow of a nanofluid past a stretching sheet. *International journal of heat and mass transfer*.53,2477-2483(2010).
- [13]. O.D. Makinde and A. Aziz. Boundary layer flow of a nanofluid past a stretching sheet with a convective boundary condition. *International journal of thermal sciences*,50,1326-1332(2011).
- [14]. K. Vajravelu, K.V. Prasad, Jinho Lee, Changhoon Lee, I. Pop, Robert A. Van Gorder. Convective heat transfer in the flow of viscous Ag-water and Cu-water nanofluids over a stretching surface. *International journal of thermal sciences*, 50,843-851(2011).
- [15]. Rafael Cortell Bataller. Effect of heat source/sink, radiation and work done by deformation on flow and heat transfer of a viscoelastic fluid over a stretching sheet. *An International journal of Computers and Mathematics with application*, 53,305-316(2007).
- [16]. G. K. Ramesh and B. J. Gireesha. Influence of heat source/sink on a Maxwell fluid over a stretching surface with convective boundary condition in the presence of nanoparticles A in *Shams Engineering Journal*, 5,991-998(2014).
- [17]. Krishnendu Bhattacharya. Effect of Heat source/sink on MHD Flow and Heat transfer over a shrinking sheet with mass suction. *Chemical Engineering Research Bulletin* 15,12-17(2011).
- [18]. G. K. Ramesh, Ali J. Chamkha and B. J. Gireesha. Magnetohydrodynamic flow of a non-Newtonian nanofluid over an impermeable surface with heat generation/absorption. *Journal of Nanofluids*, 3,78-74(2014).
- [19]. H. I. Andersson. Slip flow past a stretching surface. *Acta Mechanica*, 158, 121-125(2002).
- [20]. Wubshet Ibrahim and Bandari Shankar. MHD boundary layer flow and heat transfer of

- a nanofluid past a permeable stretching sheet with velocity, thermal and solutal slip boundary conditions. *Computers and Fluids*, 75, 1-10(2103).
- [21]. Jize Sui, Liancun Zheng and Xinxin Zhang. Boundary layer heat and mass transfer with Cattaneo-Christov double-diffusion in upper-convected Maxwell nanofluid past a stretching sheet with slip velocity. *International Journal of Thermal sciences*, 104,461-468(2016).
- [22]. B. R. Rout, S.K. Parida and S. Panda. MHD Heat and mass transfer of chemical reaction fluid flow over a moving vertical plate in presence of heat source with convective surface boundary condition. <http://dx.doi.org/10.1155/2013/296834>.
- [23]. Anjanna Matta and Nagaraju Gajjela. Order of chemical reaction and convective boundary condition effects on micropolar fluid flow over a stretching sheet. *AIP ADVANCES* 8, 115212(2018).
- [24]. Liao.S.(2003). *Beyond perturbation: Introduction to homotopy analysis method*. Chapman & Hall/CRC Press, London.
- [25]. Fan, T, & You, X. Optimal homotopy analysis method for nonlinear differential equations in the boundary layer. *Numer. Algor*,62,337-354(2013).
- [26]. Abel MS, Tawade JV, Nandeppanavar MM. MHD flow and heat transfer for the upper-convected Maxwell fluid over a stretching sheet. *Meccanica* 47,385-93(2012).
- [27]. Megahed AM. Variable fluid properties and variable heat flux effects on the flow and heat transfer in a non-Newtonian Maxwell fluid over an unsteady stretching sheet with slip velocity. *Chin Phys B* 2013;22. <http://dx.doi.org/10.1088/1674-1056/22/9/094701>.
- [28]. Abbasi FM, Mustafa M, Shehzad SA, Alhuthali MS, Hayat T. Analytical study of Cattaneo -christov heat flux model for a boundary layer flow of Oldroyd-B fluid. *Chin Phys B*,2016;25. <http://dx.doi.org/10.1088/1674-1056/25/1/014701>.

